

Isotropic superconducting state and high critical currents in $\text{Fe}_{1+y}\text{Te}_{1-x}\text{S}_x$ single crystals.

Rongwei Hu^{1,2}, J. B. Warren³ and C. Petrovic¹

¹Condensed Matter Physics and Materials Science Department,
Brookhaven National Laboratory, Upton, NY 11973

²Department of Physics, Brown University, Providence, RI 02912 and

³Instrumentation Division, Brookhaven National Laboratory, Upton, NY 11973

(Dated: July 21, 2009)

We report single crystal growth and a study of superconducting properties in $\text{Fe}_{1+y}\text{Te}_{1-x}\text{S}_x$. We demonstrate the smallest upper critical field anisotropy, $\gamma = H_{c2}^{\parallel c}/H_{c2}^{\perp c}$, among all iron based superconductors, the value of γ reaches 1.05 at $T = 0.65T_C$ for $\text{Fe}_{1.09}\text{Te}_{0.89}\text{S}_{0.11}$, while still maintaining large values of upper critical field.

The discovery of superconductivity in quaternary iron based layered superconductor $\text{LaFeAsO}_{1-x}\text{F}_x$ with $T_C = 26$ K stimulated an intense search for superconductors with higher T_C in this materials class.¹ Shortly after, the critical temperatures were raised up to 55 K in materials of the ZrCuSiAs structure type (Ref. 2), and superconductivity had been discovered in $\text{Ba}_{1-x}\text{K}_x\text{Fe}_2\text{As}$ and LiFeAs .^{3,4}

Superconductivity in the PbO - type FeSe opened another materials space in the search for iron based superconductors.⁵ This was followed by the discovery of superconductivity in $\text{FeTe}_{1-x}\text{Se}_x$ and $\text{FeTe}_{1-x}\text{S}_x$.^{6,7} Iron chalcogenide superconductors with simple binary crystal structure share the most prominent characteristics of iron arsenide compounds: a square planar lattice of Fe with tetrahedral coordination similar to LaFeAsO or LiFeAs , and Fermi surface topology.⁸ Superconducting T_C 's up to 37 K were discovered with the application of hydrostatic pressure.⁹ It was noted, however, that it would be desirable to have isotropic superconductors with high T_c and ability to carry high critical currents for power applications.¹⁰ In this work we report the synthesis of $\text{Fe}_{1+y}\text{Te}_{1-x}\text{S}_x$ ($x = 0-0.14$) superconducting single crystals. We demonstrate small values of $\gamma = H_{c2}^{\parallel c}/H_{c2}^{\perp c}$ while still maintaining large values of the upper critical field and critical currents.

Single crystals of $\text{Fe}_{1+y}\text{Te}_{1-x}\text{S}_x$ were grown from Te-S self flux using a high temperature flux method.^{11,12} Elemental Fe, Te and S were sealed in quartz tubes under partial argon atmosphere. The sealed ampoule was heated to a soaking temperature of 430-450 °C for 24h, followed by a rapid heating to the growth temperature at 850-900°C, and then slowly cooled to 800-840 °C. The excess flux was removed from crystals by decanting. Plate-like crystals up to $11 \times 10 \times 2 \text{ mm}^3$ can be grown. Elemental analysis and microstructure was performed using energy dispersive x-ray spectroscopy (EDS) in an JEOL JSM-6500 scanning electron microscope. The average stoichiometry was determined by examination of multiple points on the crystals. Powder X-ray diffraction (XRD) was measured using a Rigaku Miniflex with $\text{Cu K}\alpha$ radiation ($\lambda = 1.5418 \text{ \AA}$). The unit cell parameters were obtained by fitting the XRD spectra with the Ri-

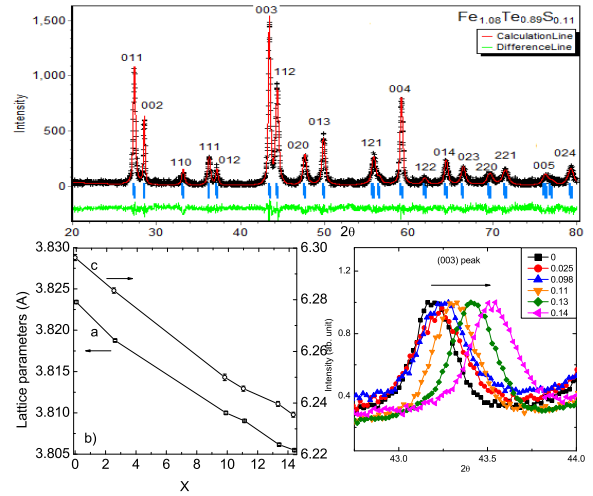


FIG. 1: Powder X-ray diffraction spectra for $x = 0$ and 0.133 samples. The lattice parameters vs. S concentration.

etika software.¹³ Flux - free rectangular shaped crystals with the largest surface orthogonal to c axis of tetragonal structure were selected for four-probe resistivity measurements. Thin Pt wires were attached to electrical contacts made with Epotek H20E silver epoxy. Sample dimensions were measured with an optical microscope Nikon SMZ-800 with $10 \mu\text{m}$ resolution. Magnetization and resistivity measurements were carried out in a Quantum Design MPMS-5 and a PPMS-9 for temperatures from 1.8 K to 350 K.

The powder X-ray diffraction patterns for all samples investigated can be indexed in the $P4/nmm$ space group of PbO structure type and small fraction of Te from the flux. Fig. 1(a) shows refinement of $\text{Fe}_{1.09}\text{Te}_{0.89}\text{S}_{0.11}$. The calculated diffraction pattern shows excellent agreement with the experiment and high phase purity. The lattice parameters are shown in Fig. 1(b). Both the a and c axis decrease uniformly with x , conforming with Vegard's law. Fig. 1(c) shows uniform evolution of $[003]$ peak with sulfur content, consistent with the decreasing c axis parameter. Thus S doping is equivalent to a positive

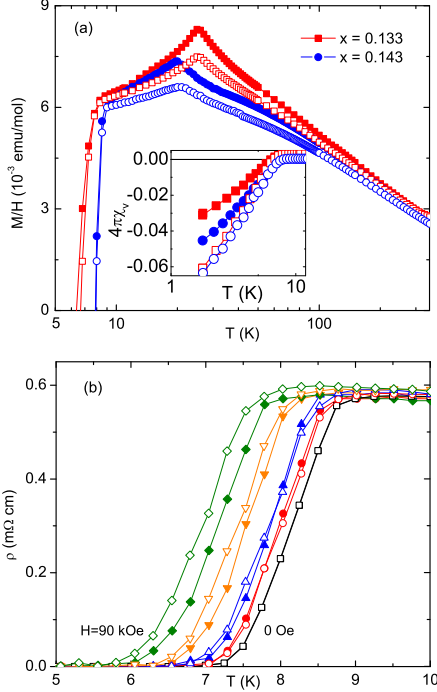


FIG. 2: a) Temperature dependence of magnetic susceptibility of two superconducting samples ($x = 0.133$ and 0.143) for $H \perp c$ (solid symbols) and $H \parallel c$ (open symbols). Inset shows the volume fraction of the as a function of temperature (1.8-12 K). b) In-plane resistivity for $x = 0.133$ of two field orientations.

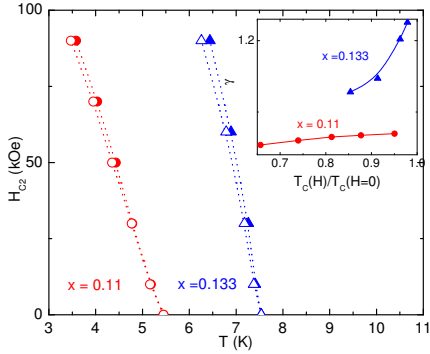


FIG. 3: The upper critical fields for $x = 0.11$ and 0.133 . Dotted lines are guides to the eye. Inset shows the anisotropy in the upper critical field $\gamma = H_{c2}^{\parallel c} / H_{c2}^{\perp c}$.

chemical pressure and reduces the unit cell volume by up to 2%. The compositions from EDS are presented in Table I. The excess Fe decreases with increasing S content.

Fig. 2 (a) shows the temperature dependence of the magnetic susceptibility for a magnetic field applied in the ab plane and along c axis. Magnetic transition is suppressed to 25 K, as was observed in $\text{FeTe}_{1-x}\text{S}_x$ polycrystals.⁷ Superconductivity is observed

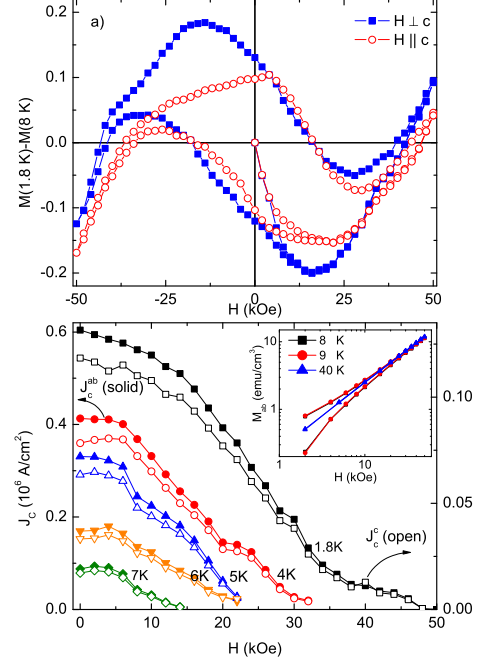


FIG. 4: a) Magnetization hysteresis loops of $x = 0.133$ for 1.8 K after ferromagnetic background subtraction for $H \parallel c$ (open symbols) and $H \perp c$ (solid symbols). b) In-plane (to left axis) and interplane (to right axis) critical currents for $x = 0.133$. Inset shows the magnetization at 8, 9 and 40 K. Only the positive field magnetization is shown on log-log scale and the virgin curves of the loops at 8 and 9 K are omitted for clarity.

for $x \geq 0.11$. The volume fraction $4\pi\chi_v$ reaches $-0.06 \sim -0.09$ at 0 K by linear extrapolation. Considering that the estimated superconducting volume fraction is only up to 10%, we speculate that the superconducting phase may exist in fractional domains associated with S atoms. With more S-doping, these domains are gradually connected to form a full superconducting path for electrical transport, as it was observed in $\text{CaFe}_{1-x}\text{Co}_x\text{AsF}$.^{14,15}

The temperature dependence of resistivity with a magnetic field applied perpendicular and parallel to c axis is shown in Fig. 2 for $x = 0.133$. The residual resistivity of the normal state $\rho_0 = 0.58 \text{ m}\Omega \text{ cm}$ of our crystals is smaller than that is observed in polycrystalline $\text{FeTe}_{1-x}\text{S}_x$.⁷ It is comparable with residual resistivity observed in $\text{NdFeAsO}_{0.7}\text{F}_{0.3}$ ($\sim 0.2 \text{ m}\Omega \text{ cm}$)¹⁶ or $(\text{Ba}_{0.55}\text{K}_{0.45})\text{Fe}_2\text{As}_2$ ($\sim 0.4 \text{ m}\Omega \text{ cm}$)¹⁷ single crystals. Transition width of our crystals ($\Delta T_c = T_{\text{onset}} - T_{\text{zerop}} = 1.8 \text{ K}$) is smaller than that in Ref. 7 ($\Delta T_c = 2 \text{ K}$). The small shift of the transition temperature with magnetic field indicates a large zero-temperature upper critical field. The upper critical field H_{c2} is estimated as the field corresponding to the 90% of resistivity drop (Fig.3). An estimate for $H_{c2}(T = 0)$ is given by weak-coupling formula for conventional superconductors

x	y	$H'_{c2}{}^{\perp c}(T_c)$	$H_{c2}{}^{\perp c}(0)(T)$	$H'_{c2}{}^{\parallel c}(T_c)$	$H_{c2}{}^{\parallel c}(0)(T)$	$\xi^{\perp c}(0)(nm)$	$\xi^{\parallel c}(0)(nm)$
0	0.15(3)						
0.110(6)	0.09(3)	-4.9	19	-4.6	18	4.3	4.3
0.133(6)	0.08(3)	-10.7	56	-8.4	44	2.4	2.7

TABLE I: EDX analysis results , upper critical field at zero temperature and corresponding coherence length.

in the Werthamer-Helfand-Hohenberg model (Table I): $H_{c2o}(0) \sim -0.7H'_{c2}(T_c)T_c$.¹⁸ The superconducting coherence length $\xi(0K)$ [$\xi^2 = \Phi_0/2\pi H_{c2}$] is around 3 nm. The anisotropy $\gamma = H_{c2}^{\parallel c}/H_{c2}^{\perp c}$ decreases with a temperature decrease approaching a value close to unity. By $T_c/T_c(0) \approx 0.65$ (Fig. 3(inset)), $\gamma = 1.05$, for $x = 0.11$. These values indicate that $FeTe_{1-x}S_x$ is a high field isotropic superconductor, with γ smaller than that in Ref. 19 ($\gamma > 1.5$ at $0.5T_C(H = 0)$) or in Ref. 20 ($\gamma \sim 1.3$ at $0.5T_C(H = 0)$).

To determine the anisotropy of the critical current, we analyze the magnetic measurements using an extended Bean model.^{21,22} Considering a rectangular prism-shaped crystal of dimension $c < a < b$, when a magnetic field is applied along the crystalline c axis, the in-plane critical current density j_c^{ab} is given by

$$j_c^{ab} = \frac{20}{a} \frac{\Delta M_c}{(1 - a/3b)}$$

in which ΔM_c is the width of the magnetic hysteresis loop for increasing and decreasing field. When the magnetic field is applied along the b axis and parallel to the ab plane, both of the in-plane j_c^{ab} and the cross-plane j_c^c are involved in the Bean model. For a crystal in our measurements with $a = 1.245mm$, $b = 1.285mm$ and $c = 0.732mm$,

$$j_c^c = \frac{c}{3a} \frac{j_c^{ab}}{(1 - 20\Delta M_b/cj_c^{ab})}$$

Because of the large volume fraction of the normal and magnetic state, a magnetic background is superposed on the hysteresis loop. Moreover, as shown in Fig. 4 (b) inset, the hysteretic magnetisation loop for the sample $x = 0.133$ sustains above the superconducting transition temperature at 7.5 K and vanishes above the antiferromagnetic transition at 25 K. It implies a magnetic struc-

ture of $FeTe_{1-x}S_x$ where a ferromagnetic component coexists with an antiferromagnetic moment. Density functional calculation on FeTe by Alaska Subedi et al does indicate that besides the SDW, FeTe is close to a ferromagnetic instability, similar to LaFeAsO.²³ In order to estimate the ΔM only due to flux pinning, we take the hysteresis loop immediately above superconducting transition at 8 K as the ferromagnetic background and subtract it from other loops below 7.5 K. The identical hysteresis loops at 8 and 9 K in the normal state justifies our rationale to use them as a temperature independent background. Fig. 4(a) shows hysteresis loops for $H//c$ and $H \perp c$ at 1.8 K after background removal. The magnetically deduced in-plane and interplane critical current density are displayed in Fig. 4(b). The ratio of j_c^{ab}/j_c^c is roughly about 4. The critical current densities for both directions are $10^5 - 10^6 A/cm^2$, comparable to MgB_2 , $Ba(Fe_{1-x}Co_x)_2As_2$ in the same temperature range²⁴.

In summary, we show that $FeTe_{1-x}S_x$ are isotropic high field superconductors with one of the smallest values of $\gamma = H_{c2}^{\parallel c}/H_{c2}^{\perp c}$ observed so far in iron based superconducting materials. Moreover, anisotropy in the superconducting state decreases with increased sulfur content. By utilizing high pressure synthesis techniques even higher T_C 's, upper critical fields and smaller γ may be simultaneously obtained. Since $FeTe_{1-x}S_x$ superconductors consist of relatively inexpensive and nontoxic elements they may represent future materials of choice for high field power applications.

We thank Paul Canfield, Sergey Bud'ko and Myron Strongin for useful discussions. This work was carried out at the Brookhaven National Laboratory, which is operated for the U.S. Department of Energy by Brookhaven Science Associates (DE-Ac02-98CH10886). This work was supported by the Office of Basic Energy Sciences of the U.S. Department of Energy.

¹ Y. Kamihara, T. Watanabe, M. Hirano, and H. Hosono, J. Am. Chem. Soc. **130**, 3296 (2008).

² Z. A. Ren, L. U. Wei, Jie Yang, Y. Wei, Xiao-Li Shen, Zheng-Cai Li, Guang-Can Che, Xiao-Li Dong, Li-Ling Sun, Fang Zhou and Zhong-Xian Zhao, Chinese Phys. Lett. **25**, 2215 (2008).

³ Marianne Rotter, Marcus Tegel and Dirk Johrendt, Phys. Rev. Lett. **101**, 107006 (2008)

⁴ X.C.Wang, Q.Q. Liu, Y.X. LV, W.B. Gao, L.X.Yang, R.C.

Yu and F.Y.Li, C.Q. Jin, Solid State Communications 148, 538 (2008)

⁵ Fong-Chi Hsu, Jiu-Yong Luo, Kuo-Wei Yeh, Ta-Kun Chen, Tzu-Wen Huang, Phillip M. Wu, Yong-Chi Lee, Yi-Lin Huang, Yan-Yi Chu, Der-Chung Yan, and Maw-Kuen Wu, Proc. Natl. Acad. Sci. U.S.A. **105**, 14262 (2008).

⁶ K. W. Yeh, T. W. Huang, Y. L. Huang, T. K. Chen, F. C. Hsu, Phillip M. Wu, Y. C. Lee, Y. Y. Chu, C.L. Chen, J. Y. Luo, D. C. Yan and M. K. Wu, Europhys. Lett. **84**,

- 37002 (2008).
- ⁷ Yoshikazu Mizuguchi, Fumiaki Tomioka, Shunsuke Tsuda, Takahide Yamaguchi and Yoshihiko Takano, *Appl. Phys. Lett.* **94**, 012503 (2009).
 - ⁸ Lijun Zhang, D. J. Singh, and M. H. Du, *Phys. Rev. B* **79**, 012506 (2009).
 - ⁹ S. Margadonna, Y. Takabayashi, Y. Ohishi, Y. Mizuguchi, Y. Takano, T. Kagayama, T. Nakagawa, M. Takata and K. Prassides, e-print arXiv:0903.2204.
 - ¹⁰ Report on of the Basic Energy Sciences, US Department of Energy, Superconductivity, (Washington, DC, United States), 2006.
 - ¹¹ P. C. Canfield, *Z. Fisk Phil. Magaz. B* **65**, 1117 (1992).
 - ¹² Z. Fisk, J. P. Remeika, in: K. A. Gschneider, J. Eyring (Eds.), *Handbook on the Physics and Chemistry of Rare Earths*, Vol. **12**, Elsevier, Amsterdam, (1989).
 - ¹³ 12B. Hunter, “RIETICA—A Visual RIETVELD Program,” International Union of Crystallography Commission on Powder Diffraction Newsletter No. 20 Summer , 1998 <http://www.rietica.org>
 - ¹⁴ Y. Xiao, Y. Su, R. Mittal, T. Chatterji, T. Hansen, C.M.N. Kumar, S. Matsuishi, H. Hosono, Th. Brueckel, *Phys. Rev. B* **79**, 060504(R) (2009).
 - ¹⁵ S. Takeshita, R. Kadono, M. Hiraishi, M. Miyazaki, A. Koda, S. Matsuishi, and H. Hosono, arXiv:0812.1670.
 - ¹⁶ J. Jaroszynski, F. Hunte, L. Balicas, Youn-jung Jo, I. Raičević, A. Gurevich, D. C. Larbalestier, F. F. Balakirev, L. Fang, P. Cheng, Y. Jia, and H. H. Wen, *Phys. Rev. B* **78**, 174523 (2008)
 - ¹⁷ N. Ni, S. L. Bud’ko, A. Kreyssig, S. Nandi, G. E. Rustan, A. I. Goldman, S. Gupta, J. D. Corbett, A. Kracher, and P. C. Canfield, *Phys. Rev. B* **78**, 014507 (2008)
 - ¹⁸ N. R. Werthamer, E. Helfand, and P. C. Hohenberg, *Phys. Rev.* **147**, 295 (1966).
 - ¹⁹ A. Yamamoto, a J. Jaroszynski, C. Tarantini, L. Balicas, J. Jiang, A. Gurevich, D. C. Larbalestier, R. Jin, A. S. Sefat, M. A. McGuire, B. C. Sales, D. K. Christen, and D. Mandrus, *Appl. Phys. Lett.*, **94**, 062511 (2009)
 - ²⁰ S. A. Baily, Y. Kohama, H. Hiramatsu, B. Maiorov, F. F. Balakirev, M. Hirano, and H. Hosono, *Phys. Rev. Lett.* **102**, 117004 (2009)
 - ²¹ C. P. Bean, *Phys. Rev. Lett.* **8**, 250 (1962).
 - ²² E. M. Gyorgy, R. B. van Dover, K. A. Jackson, L. F. Schneemeyer and J. V. Waszczak, *Appl. Phys. Lett.*, **55**, 283 (1989)
 - ²³ Alaska Subedi, Lijun Zhang, D. J. Singh, and M. H. Du, *Phys. Rev. B* **78**, 134514 (2008)
 - ²⁴ M. A. Tanatar, N. Ni, C. Martin, R. T. Gordon, H. Kim, V. G. Kogan, G. D. Samolyuk, S. L. Bud’ko, P. C. Canfield, and R. Prozorov, *Phys. Rev. B* **79**, 094507 (2009)